# Microbial Competition: Study of Global Branching Phenomena

**Abdelhamid Ajbar and Khalid Alhumazi**
Dept. of Chemical Engineering, King Saud University, Riyadh 11421, Saudi Arabia

*The stability characteristics of a bioreactor with cell recycle involving the competition between microbial cultures are investigated. The unstructured model, based on Andrew's inhibitory kinetics, involves the pure and simple competition between two microorganisms for a single pollutant. The singularity theory used for this study allows an in-depth analysis of both the static and dynamic bifurcation mechanisms occurring in the system. The hysteresis with five solutions is the highest singularity the system can exhibit. With inhibitory kinetic expressions, the model can also predict self-sustained oscillations for a wide range of parameters. The analysis of clean feed conditions shows that the model cannot exhibit periodic behavior regardless of the growth kinetics model. Analytical criteria are also derived for the coexistence of the competing cultures and for the prevention of wash-out conditions. The stability characteristics for Monod kinetics, derived as a limiting case of the inhibitory kinetic expressions, are incorporated in the general framework offered by the singularity theory.*

## Introduction

The dynamics and stability characteristics of the continuous stirred tank bioreactor (CSTBR) have been the subject of a number of theoretical and experimental investigations (Di-Biasio et al., 1981; Agrawal et al., 1982; Baltzis et al., 1989; Bertucco et al., 1989; Lenas and Pavlou, 1992; Ajbar and Ibrahim, 1997a,b). These studies have shown that the CSTBR with or without cell recycle is capable of exhibiting a wide range of nonlinear phenomena. Among such phenomena are the occurrence of steady-state multiplicity, self-sustained oscillations, and even chaotic behavior. The use of bioreactors in the treatment of domestic and industrial liquid wastes is an established technology; nevertheless, it is expected that a continuous understanding of the kinetics of the biodegradation, the interactions between microbial populations and the dynamics of the bioreactor employed in the process can lead to more efficient reactor technologies and better modes of operations. In this regard an interesting class of biological treatment processes concerns the competition arising among microbial populations inhabiting a common environment. Microbial competition plays an important part in biological wastewater treatment processes and also plays a significant role in the biological dynamics of natural ecosystems. For these reasons, the study of the dynamics of competing microbial populations is important for the operation of the bioreactor, for scale-up of biodegradation data, and is particularly useful in applications where a biomass of specific compositions is desired.

Pure and simple competition, where microbial populations interact in no other way and expect competition for a single rate-limiting nutrient, was studied for years both theoretically and experimentally (Aris and Humphrey, 1977; Fredrickson and Stephanopoulos, 1981; Baltzis and Fredrickson, 1983, 1984; Matsubara et al., 1986; Powell, 1988; Pavlou and Kevrekidis, 1992; Dikshitulu et al., 1993; Smith and Waltman, 1995). These studies, carried out under conditions of constant and periodically varied feed conditions, have revealed parts of the richness of the dynamics of competition. Two microbial cultures, engaged in pure and simple competition, can introduce phenomena of multiplicity in the chemostat for some range of dilution rates (Aris and Humphrey, 1977). It is also established that two competing cultures, under ideal mixing and time invariant inputs, cannot coexist except at discrete values of the chemostat dilution rate (Aris and Humphrey, 1977; Hsu, 1978; Hansen and Hubbell, 1980; Baltzis and Fredrickson, 1983, 1984; Butler and Wolkowicz,

Correspondence concerning this article should be addressed to K. Alhumazi.

1985). This coexistence, however, is not structurally stable because of inevitable random fluctuations in the feed conditions (Stephanopoulos et al., 1979a; Powell, 1988). When the feed conditions are on the other hand periodically varied, two competing populations were proved to coexist not only in a state of limit cycle (Stephanopoulos et al., 1979b; Hsu, 1980; Hale and Somolinos, 1983; Mastubara et al., 1986; Pavlou et al., 1990), but also in quasiperiodic states as well as in chaotic state (Lenas and Pavlou, 1992).

In the present work, the problem of pure and simple competition in a bioreactor with cell recycle and under time-invariant feed conditions is revisited. Two objectives are sought from this study. The first objective is to provide a unified framework, using the singularity theory, for the analysis of static bifurcation induced in the bioreactor by the competing cultures. The relative simplicity of the reactor-settler model allows the description of the steady-state behavior of the bioreactor in the form of a single algebraic equation. The singularity theory can provide a general framework and a powerful tool for classifying branching phenomena in which different kinds of multiplicity in the nonlinear model of the bioreactor can be expected. It is shown that a general and practical picture of the different stability phenomena in the reactor, including different types of steady-state multiplicity and modes of coexistence, can be drawn in a systematic and quite useful manner. The relative simplicity of the resulting steady-state equation makes the analysis even more useful, since closed analytical results can be obtained to describe the different conditions for the existence of multiplicity and for the coexistence of the competing cultures.

Many of the related results about the singularity theory are attributed to Golubitsky and Schaeffer (1985). The theory has found several applications in chemical engineering since Balakotaiah and Luss (1982) analyzed the multiplicity phenomenon of the simple CSTR. D'anna et al. (1986) and Alhumazi and Aris (1995) provided other applications of the theory in their study of the stability characteristics of autocatalytic reactive systems. Ajbar and Ibrahim (1997a), on the other hand, applied the theory to analyze the different branching phenomena in the basic unstructured model of the CSTBR with cell recycle. Most of the related materials about the theory can be found in the referenced textbook (Golubitsky and Schaeffer, 1985) or in the useful summaries provided by Alhumazi and Aris (1995).

The second objective of this article is to study the dynamic bifurcation induced by the competing cultures. In contrast to linear systems, it is known that structurally stable periodic solutions can exist for nonlinear systems. The ability of the bioreactor model to predict coexistence of the competing populations in an oscillatory mode is investigated. The combination of results of both static and dynamic analysis helps to draw a complete picture of the different modes of behavior induced in the bioreactor by the competing cultures.

An unstructured model of the bioreactor with cell recycle is used to describe the microbial competition. The use of recycle makes the study pertinent to potential applications in the area of biological treatment of wastewater. However, it is shown that the general treatment offered by the singularity theory can be extended to clean feed case, a much more practical application. The Andrew's kinetic expression (Andrews, 1968) with three adjustable parameters is selected to describe substrate inhibition effects associated with the growth of the two cultures. It is shown that the stability characteristics in the case of noninhibitory (Monod) growth kinetics can be derived as a limiting case of the Andrew's expressions, and are therefore readily incorporated within the general treatment offered, in this work, by the singularity theory. Finally, to ensure that simulations reflect a real biological system, the values of the model kinetic parameters, when used, are taken from the experimental work of Dikshitulu et al. (1993) for the growth of pure cultures of *Pseudomonas putida* and *Pseudomonas resinovorans* in a media containing phenol.

The model of the reactor-settler unit is presented. Static and dynamic bifurcation analysis for the general case are carried out, followed by the analysis of the stability characteristics for the case of clean feed conditions. Finally, the dynamics of the unit with Monod growth kinetics are studied.

## Process Model

We consider the bioreactor with cell recycle shown in Figure 1. Two microbial populations ($X_1$) and ($X_2$) are capable of growing on the substrate ($S$). The purge fraction $W$ containing the biomass is operated directly from the reactor and ideal conditions are assumed to prevail in the settler. The unsteady-state mass balances for the different species are established in the following.

### *Substrate S*

The mass balance for substrate $S$ is given by

$$QS_f + QRS - \frac{r_1 X_1 V}{Y_1} - \frac{r_2 X_2 V}{Y_2} = QWS + Q(1 + R - W)S + V\frac{dS}{dt} \quad (1)$$

where $r_1$ and $r_2$ are the specific growth rates associated respectively with $X_1$ and $X_2$. Equation 1 yields

$$S_f - S - \theta\left(\frac{r_1 X_1}{Y_1} + \frac{r_2 X_2}{Y_2}\right) = \theta\frac{dS}{dt} \quad (2)$$

where $\theta = V/Q$ is the reactor residence time.

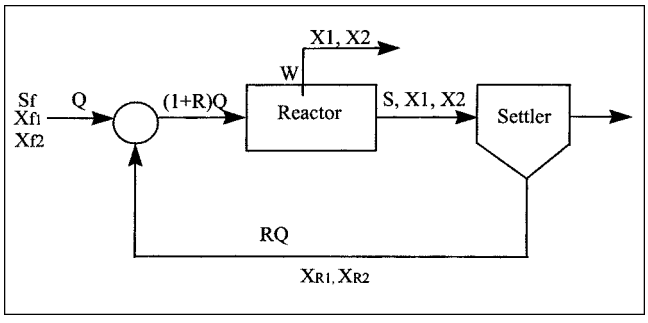


**Figure 1. Bioreactor with cell recycle.**

*Biomass of $X_1$*

The mass balance for $X_1$ is given by

$$QX_{f_1} + RQX_{R_1} + r_1 X_1 V = Q(1+R)X_1 + V\frac{dX_1}{dt} \qquad (3)$$

Ideal conditions in the settler allow the following simple relation between the exit biomass $X_1$ and the recycle biomass $X_{R_1}$ concentrations

$$X_{R_1} = X_1\left(\frac{1+R-W}{R}\right) \qquad (4)$$

Substituting in Eq. 3 for the recycle biomass concentrations yields

$$X_{f_1} - WX_1 + \theta r_1 X_1 = \theta\frac{dX_1}{dt} \qquad (5)$$

*Biomass of $X_2$*

The mass balance for the biomass of $X_2$ is similar to Eq. 5

$$X_{f_2} - WX_2 + \theta r_2 X_2 = \theta\frac{dX_2}{dt} \qquad (6)$$

The two competing cultures $X_1$ and $X_2$ grow on substrate $S$ following Andrew's inhibitory expressions

$$r_j = \frac{\mu_j S}{K_j + S + S^2/K_{I_j}} \quad j = 1,2 \qquad (7)$$

The mass balances are suitably rendered dimensionless using the variables shown in Table 1. The dimensionless mass balance equations for the different species are then

$$\bar{S}_f - \bar{S} - \bar{\theta}\left(\bar{r}_1\bar{X}_1 + \eta\bar{r}_2\bar{X}_2\right) = \frac{d\bar{S}}{d\bar{t}} \qquad (8)$$

$$\bar{X}_{f_1} - W\bar{X}_1 + \bar{\theta}\bar{r}_1\bar{X}_1 = \frac{d\bar{X}_1}{d\bar{t}} \qquad (9)$$

$$\bar{X}_{f_2} - W\bar{X}_2 + \bar{\theta}\bar{r}_2\bar{X}_2 = \frac{d\bar{X}_2}{d\bar{t}} \qquad (10)$$

The dimensionless expressions of the specific growth rates are given, on the other hand, by

$$\bar{r}_1 = \frac{\bar{S}}{1+\bar{S}+\gamma_1\bar{S}^2} \quad \text{and} \quad \bar{r}_2 = \frac{\phi\bar{S}}{\alpha+\bar{S}+\gamma_2\bar{S}^2} \qquad (11)$$

**Table 1. Dimensionless Variables Used in the Model**

| Parameter | Definition | Parameter | Definition |
|---|---|---|---|
| $\bar{\theta}$ | $\mu_1\theta$ | $\alpha$ | $K_2/K_1$ |
| $\bar{S}$ | $S/K_1$ | $\gamma_1$ | $K_1/K_{I_1}$ |
| $\bar{t}$ | $t/\theta$ | $\gamma_2$ | $K_1/K_{I_2}$ |
| $\bar{X}_1$ | $X_1/(Y_1K_1)$ | $\eta$ | $Y_1/Y_2$ |
| $\bar{X}_2$ | $X_2/(Y_1K_1)$ | $\phi$ | $\mu_2/\mu_1$ |

The noninhibitory (Monod) growth model is obtained as a limiting case of Eq. 11 as the dimensionless inhibition constants $\gamma_1$ and $\gamma_2$ take on small values, that is, $\gamma_j \to 0$, $j = 1, 2$.

The steady-state equations are obtained by setting the left-hand sides of Eqs. 8–10 to zero. Equations 9–10 in particular would yield

$$\bar{X}_1 = \frac{\bar{X}_{f_1}}{W - \bar{r}_1\bar{\theta}} \quad \text{and} \quad \bar{X}_2 = \frac{\bar{X}_{f_2}}{W - \bar{r}_2\bar{\theta}} \qquad (12)$$

By introducing Eqs. 12 into the steady-state form of Eq. 8, an algebraic equation is obtained for $\bar{S}$,

$$F(\bar{S}) := \bar{S}_f - \bar{S} - \bar{\theta}\left(\frac{\bar{r}_1\bar{X}_{f_1}}{W - \bar{r}_1\bar{\theta}} + \eta\frac{\bar{r}_2\bar{X}_{f_2}}{W - \bar{r}_2\bar{\theta}}\right) \qquad (13)$$

Substituting in Eq. 13 for the expressions of $\bar{r}_1$ and $\bar{r}_2$ (Eq. 11), a single fifth-order polynomial is obtained for the substrate concentration $\bar{S}$

$$F(\bar{S}) := a_5\bar{S}^5 + a_4\bar{S}^4 + a_3\bar{S}^3 + a_2\bar{S}^2 + a_1\bar{S} + a_0 = 0 \qquad (14)$$

The coefficient $a_i$ is listed in Table 2. Another useful equation can be obtained by multiplying the steady-state form of Eq. 10 by $(\eta)$ and adding it to Eqs. 8–10, which yields

$$\bar{S}_f - \bar{S} + \left(\bar{X}_{f_1} + \eta\bar{X}_{f_2}\right) - W\left(\bar{X}_1 + \eta\bar{X}_2\right) = 0 \qquad (15)$$

The steady states of the model are therefore bounded. The substrate concentration $\bar{S}$ is bounded obviously by the feed condition $\bar{S}_f$, while the maximum concentration of the biomass is obtained by setting $\bar{S} = 0$ in Eq. 15 which yields

$$\bar{X}_1 + \eta\bar{X}_2 = \frac{1}{W}\left(\bar{S}_f + \bar{X}_{f_1} + \eta\bar{X}_{f_2}\right) \qquad (16)$$

We are interested in the way the steady-state $\bar{S}$ depends on the positive system parameters. The residence time appearing explicitly in the coefficients of Eq. 14 is the easiest parameter to vary and is selected to be the bifurcation parameter. The steady-state equation (Eq. 14) is of the fifth-order in $\bar{S}$, so for a given value of $\bar{\theta}$, a maximum five steady-state solutions are possible. For this kind of equation, the singular-

**Table 2. Coefficients of the Polynomial $F(\bar{S}) := a_5\bar{S}^5 + a_4\bar{S}^4 + a_3\bar{S}^3 + a_2\bar{S}^2 + a_1\bar{S} + a_0 = 0$**

$$a_0 := \alpha\bar{S}_f W^2$$

$$a_1 := -\bar{\theta}W\bar{S}_f(\alpha+\phi) - \bar{\theta}W(\alpha\bar{X}_{f_1} + \eta\phi\bar{X}_{f_2}) + W^2(\alpha\bar{S}_f + \bar{S}_f - \alpha)$$

$$a_2 := \phi\bar{S}_f\bar{\theta}^2 + \bar{\theta}W(\alpha+\phi-\bar{S}_f-\phi\bar{S}_f) + W^2(\gamma_2\bar{S}_f + \alpha\gamma_1\bar{S}_f + \bar{S}_f - \alpha - 1) + \phi\bar{\theta}^2(\bar{X}_{f_1} + \eta\bar{X}_{f_2}) - \bar{\theta}W(\bar{X}_{f_1} + \eta\phi\bar{X}_{f_2})$$

$$a_3 := -\phi\bar{\theta}^2 + \bar{\theta}W(1+\phi) - \bar{\theta}W\bar{S}_f(\gamma_2+\phi\gamma_1) - \bar{\theta}W(\gamma_2\bar{X}_{f_1} + \gamma_1\eta\phi\bar{X}_{f_2}) + W^2(-\gamma_2 + \gamma_1\bar{S}_f + \gamma_2\bar{S}_f - \alpha\gamma_1 - 1)$$

$$a_4 := \bar{\theta}W(\gamma_2+\phi\gamma_1) - W^2(\gamma_1+\gamma_2) + \gamma_1\gamma_2\bar{S}_f W^2$$

$$a_5 := -\gamma_1\gamma_2 W^2$$

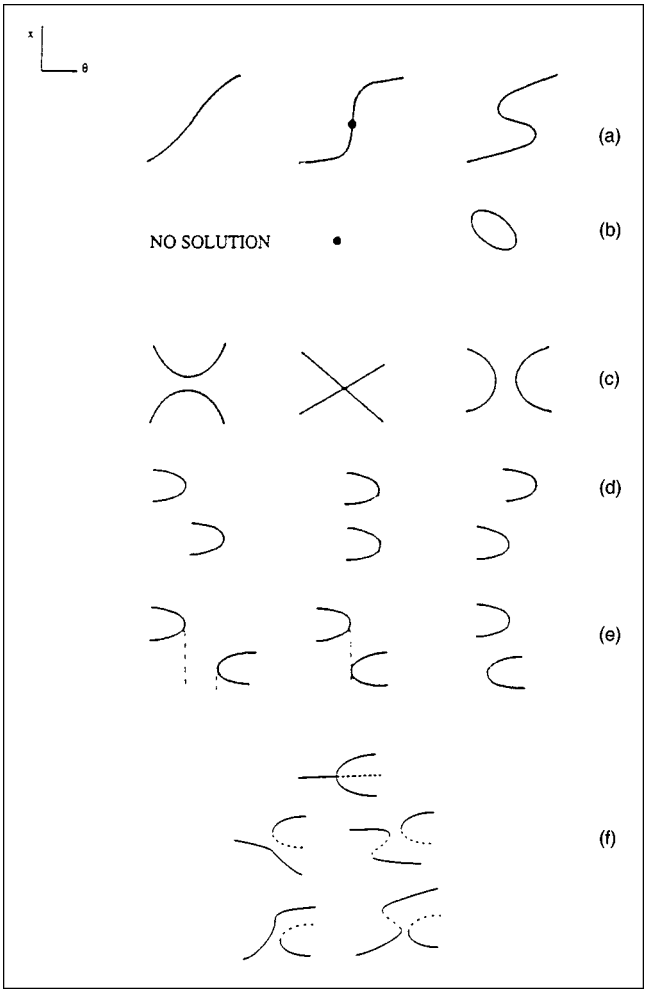


**Figure 2. Examples of singularities: (a) hysteresis; (b) isola; (c) mushroom; (d)–(e) double limit; (f) pitchfork.**

ity theory defines two types of codimension-one singularities that can be found, namely hysteresis (Figure 2a), isola-mushroom (Figures 2b–2c) and double limit (Figures 2d–2e). Pitchfork (codimension-two) (Figure 2f) singularity is also defined for a fifth-order polynomial.

## Static Bifurcation

### *Hysteresis singularity*

The conditions for the appearance/disappearance of a hysteresis loop are

$$F = F_{\bar{S}} = F_{\bar{S}\bar{S}} = 0 \tag{17}$$

that is, the point should be a steady-state point ($F = 0$) and the first two partial derivative of $F$ with respect to $\bar{S}$ must vanish. In addition a number of other derivatives must remain non-zero, namely, $F_{\bar{\theta}}$, $F_{\bar{S}\bar{\theta}}$ and $F_{\bar{S}\bar{S}\bar{S}}$.

The above conditions form the boundaries for the hysteresis singularity. Before we establish these boundaries, a simple analysis can be carried out to determine the conditions for the first derivative $F_{\bar{S}}$ to vanish, since it is also a requirement for the existence of a static limit point (SLP), that is, multiplicity. Using the expression of $F$ in Eq. 13, it can be seen that the first derivative $F_{\bar{S}}$ is such that

$$-F_{\bar{S}} = 1 + \bar{\theta} W \bar{X}_{f_1} \frac{\bar{r}_1'}{\left(W - \bar{r}_1 \bar{\theta}\right)^2} + \bar{\theta} W \eta \bar{X}_{f_2} \frac{\bar{r}_2'}{\left(W - \bar{r}_2 \bar{\theta}\right)^2} \tag{18}$$

where $\bar{r}_i'$, $i = 1, 2$ are the first derivatives of $\bar{r}_i$. From Eq. 18, it can be seen that, for the condition $F_{\bar{S}} = 0$ to be satisfied, it is necessary that either $\bar{r}_1'$ or $\bar{r}_2'$ are negatives. Recall that

$$\bar{r}_1' = \frac{1 - \gamma_1 \bar{S}^2}{\left(1 + \bar{S} + \gamma_1 \bar{S}^2\right)^2} \quad \text{and} \quad \bar{r}_2' = \frac{\phi\left(\alpha - \gamma_2 \bar{S}^2\right)}{\left(\alpha + \bar{S} + \gamma_2 \bar{S}^2\right)^2} \tag{19}$$

The necessary conditions for the occurrence of static limit points are then

$$\frac{1}{\gamma_1} \le \bar{S}^2 \quad \text{or} \quad \frac{\alpha}{\gamma_2} \le \bar{S}^2 \tag{20}$$

Since $\bar{S}$ is always bounded by the feed condition $\bar{S}_f$, it is necessary then to have

$$\gamma_1 \bar{S}_f^2 \ge 1 \quad \text{or} \quad \frac{\gamma_2}{\alpha} \bar{S}_f^2 \ge 1 \tag{21}$$

With these conditions established, the set of nonlinear equations (Eq. 17) can be solved to determine the limits of the hysteresis regions. The numerical simulations are carried out using the nominal values of the kinetic parameters (Dikshitulu et al., 1993) and the bioreactor operating parameters, shown in Table 3.

**Table 3. Nominal Kinetic (Dikshitulu et al., 1993) and Operating Parameters Used in Simulations**

| Parameter | Value | Parameter | Value |
|---|---|---|---|
| $\alpha$ | 1.063995 | $\bar{S}_f$ | 6 |
| $\gamma_1$ | 0.059918 | $\bar{X}_{f_1}$ | 0.001 |
| $\gamma_2$ | 0.103665 | $\bar{X}_{f_2}$ | 0.001 |
| $\eta$ | 1.137778 | $W$ | 0.1 |
| $\phi$ | 1.122631 | | |

Figures 3a–3c show the hysteresis boundaries in the parameter spaces ($\bar{S}_f$, $\bar{X}_{f_1}$), ($\bar{S}_f$, $X_{f_2}$), and ($\bar{S}_f$, $W$). The conditions $F_{\bar{\theta}}$, $F_{\bar{S}\bar{\theta}}$ and $F_{\bar{S}\bar{S}\bar{S}}$ were evaluated numerically along the hysteresis surface, and no point was found to violate the conditions. When crossing the boundaries in Figures 3a–3c, the number of static limit points in the bifurcation diagrams increase/decrease by two. The boundaries in Figure 3a, for instance, divide the parameter space in three regions. Region a is characterized, for any combinations of ($\bar{S}_f$, $\bar{X}_{f_1}$), by the absence of static limit points, that is, unique steady-state solution. The expected behavior in this region is shown in the

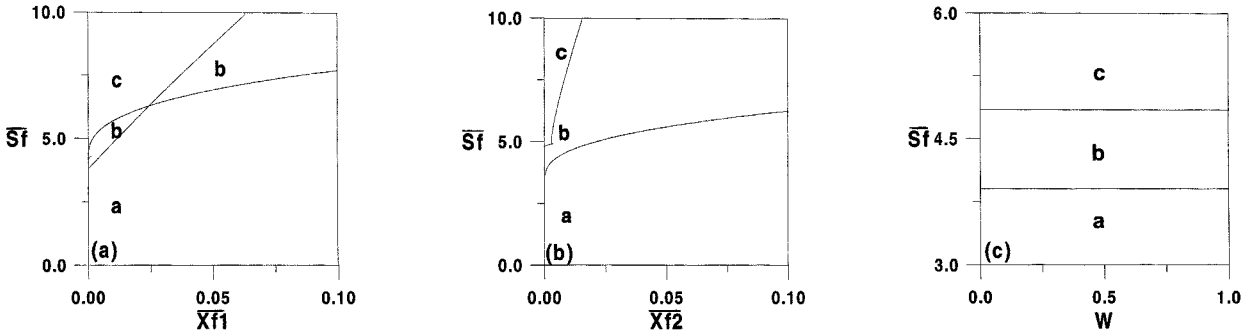


**Figure 3. Branch sets for the hysteresis singularity.**

continuity diagram of Figure 4a obtained, for example, with $(\bar{S}_f, \bar{X}_{f_1}) = (3.5, 0.003)$. The software package of Doedel and Kernevez (1986) was used to generate the continuity diagrams. When crossing the boundary separating regions a and b, two static limit points are born. A hysteresis with a maximum three steady-state solutions characterize the nature of the system in region b. Figure 4b shows an example of the behavior in this region obtained with $(\bar{S}_f, \bar{X}_{f_1}) = (4.5, 0.003)$. The upper stable branch corresponds to low conversion, while high conversion conditions are possible on the lower branch. Region c on the other hand is characterized by the presence of four limit points since two extra SLP are born when crossing the boundary between regions b and c. A maximum of five steady-state solutions are expected in this region, as it can be seen in the continuity diagram of Figure 4c obtained with $(\bar{S}_f, \bar{X}_{f_1}) = (5.6, 0.001)$. In addition to stable low and high conversion branches, a third stable branch exists in the middle. In all these cases, hysteresis introduces dangerous operations for the reactor since any abrupt change in the operating parameters can cause the system to jump from high conversion points to low conversion operating points. Experimental evidence of the hysteresis behavior was reported in early studies of bioreactors (DiBiasio et al., 1981). The same three modes of behavior are found in the parameter space $(\bar{S}_f, \bar{X}_{f_2})$ (Figure 3b). The effect of the purge fraction, on the other hand, can be seen in Figure 3c. Although the same modes of behavior exist, it can be seen that the hysteresis boundaries are insensitive to changes in the purge fraction. Therefore, when the other operating parameters are invariant, a change in the recycle ratio has no effect on the static behavior of the bioreactor.

### *Double limit singularity*

The existence of four static limit points in the model is an indication of potential richness, since the relative location of the limit points can change in the bifurcation diagrams. A typical example of this behavior is provided by the double limit singularity (Figures 2d–2e), where the number of static limit points does not change but their relative positions do. This singularity is defined by the following relations

$$F(\bar{S}_1) = F(\bar{S}_2) = 0 \tag{22}$$

and

$$F_{\bar{S}}(\bar{S}_1) = F_{\bar{S}}(\bar{S}_2) = 0 \tag{23}$$

with

$$\bar{S}_1 \neq \bar{S}_2 \tag{24}$$

These relations require that two distinct points $\bar{S}_1$ and $\bar{S}_2$ should satisfy steady state and also limit point conditions.

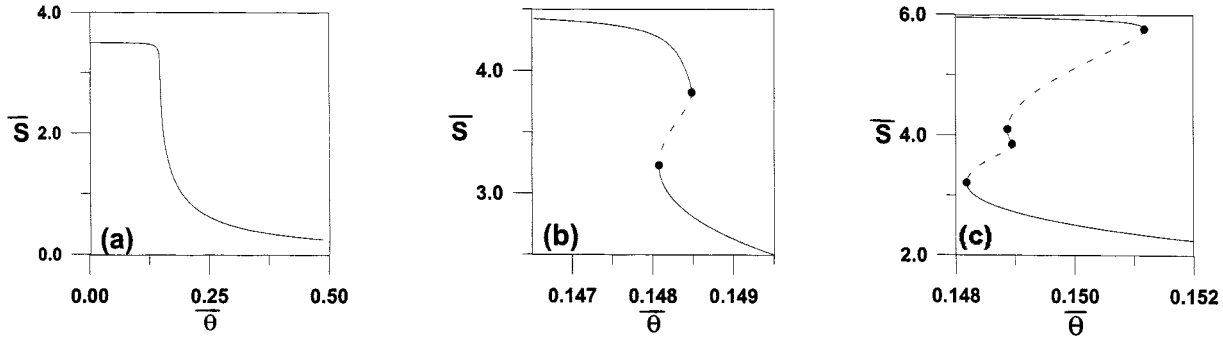


**Figure 4. Continuity diagrams for the different regions of Figure 3a.**

(a) Unique solution in region (a); (b) maximum three solutions in region (b); (c) maximum five solutions in region (c); ——: stable branch; – – –: unstable; ●: static limit point.

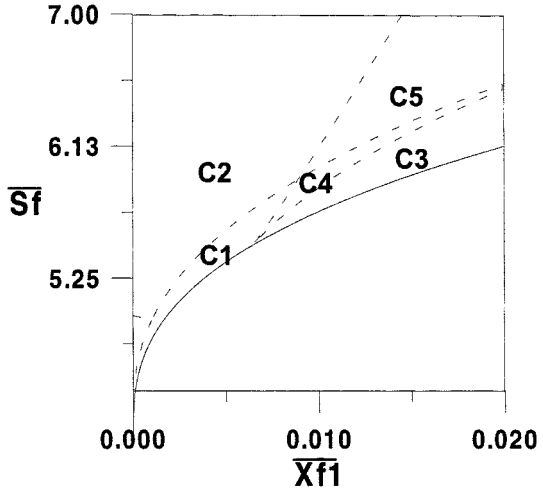


**Figure 5. Branch sets for the double limit singularity.**

——: Boundary for the hysteresis singularity with four static limit points; – – –: boundaries for the double limit singularity.

Figure 5 shows the boundaries of the double limit singularity in the parameter space $(\bar{S}_f, \bar{X}_{f_1})$. The region of four static limit points (region c in Figure 3a) can in fact be divided in five different subregions. Figures 6 $(c_1 - c_5)$ show the various behavior expected. All these regions predict five steady-state solutions in a small or large range of residence time, except region $c_5$ (Figure 6), where the maximum number of steady-state solutions at any residence time is three.

### *Isola and mushroom*

The third possible qualitative change that can occur in the steady-state locus is the appearance of an isola (Figure 2b) and the growth of an isola into a mushroom (Figure 2c). The requirements for these two changes in the steady-state behavior are that

$$F = F_{\bar{S}} = F_{\bar{\theta}} = 0 \tag{25}$$

with the additional requirements that

$$F_{\bar{S}\bar{\theta}} \neq 0, \quad F_{\bar{S}\bar{S}} \neq 0, \quad F_{\bar{\theta}\bar{\theta}} \neq 0 \tag{26}$$

Taking the derivative of $F$ (Eq. 13) with respect to $\bar{\theta}$ yields

$$-F_{\bar{\theta}} = \frac{\bar{r}_1 \bar{X}_{f_1} W}{\left(W - \bar{r}_1 \bar{\theta}\right)^2} + \frac{\bar{r}_2 \bar{X}_{f_2} W}{\left(W - \bar{r}_2 \bar{\theta}\right)^2} \tag{27}$$

Since all the terms involved in these equations are positive, the requirement that $F_{\bar{\theta}} = 0$ implies necessarily that either one of the following conditions are satisfied

$$\bar{r}_1 = 0 \quad \text{and} \quad \bar{r}_2 = 0 \tag{28}$$

or

$$\bar{X}_{f_1} = 0 \quad \text{and} \quad \bar{X}_{f_2} = 0 \tag{29}$$

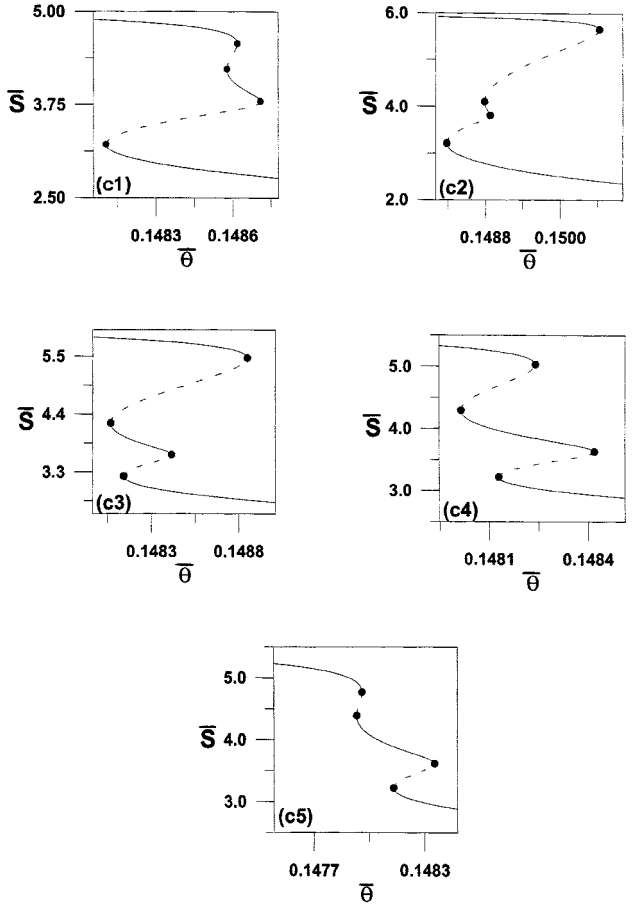


**Figure 6. Continuity diagrams for the different regions of Figure 5.**

——: Stable branch; – – –: unstable; ●: static limit point.

The first conditions are satisfied for the case of $\bar{S} = 0$, while the second conditions correspond to clean feed conditions. However, both these conditions would violate the requirement that $F_{\bar{\theta}\bar{\theta}} \neq 0$ since

$$F_{\bar{\theta}\bar{\theta}} = \frac{2\bar{X}_{f_1}\bar{r}_1^2 W}{\left(W - \bar{r}_1\bar{\theta}\right)^3} + \frac{2\bar{X}_{f_2}\bar{r}_2^2 W}{\left(W - \bar{r}_1\bar{\theta}\right)^3} \tag{30}$$

vanishes exactly at these conditions. The model cannot therefore exhibit an isola or mushroom singularity.

### *Pitchfork singularity*

In order for the single scalar function to undergo a pitchfork bifurcation (Figure 2f), it is sufficient to have

$$F = F_{\bar{S}} = F_{\bar{\theta}} = F_{\bar{S}\bar{S}} = 0 \tag{31}$$

and

$$F_{\bar{S}\bar{\theta}} \neq 0, \quad F_{\bar{S}\bar{S}\bar{S}} \neq 0 \tag{32}$$

Under these conditions, the function $F$ is equivalent to a pitchfork normal form. Since the condition of the existence

of a pitchfork includes the condition $F_{\bar{\theta}} = 0$ as in the case of isola and mushroom, it is clear that the only possible cases where the system can predict a pitchfork are those of conditions (Eqs. 28–29). For the case $\bar{S} = 0$, the first derivatives of the rates, from Eq. 19, are $r_1' = 1$ and $r_2' = \phi/\alpha$. Since both these terms are positive, the condition $F_{\bar{S}} = 0$ cannot be satisfied. Moreover, the derivative with respect to $\bar{S}$ of $F_{\bar{\theta}}$ (Eq. 27) yields

$$-F_{\bar{S}\bar{\theta}} = W\bar{X}_{f_1}\left[\frac{\bar{r}_1}{\left(W-\bar{r}_1\bar{\theta}\right)^2}\right]' + W\bar{X}_{f_2}\left[\frac{\bar{r}_2 W}{\left(W-\bar{r}_2\bar{\theta}\right)^2}\right]' \quad (33)$$

It is clear that the condition $F_{\bar{S}\bar{\theta}} \neq 0$ is violated at the clean feed conditions.

The model cannot therefore exhibit codimension two singularity or a higher one.

The analysis of the state bifurcation has revealed that hysteresis with a maximum of five solutions is the highest singularity the model can predict. In the next section we carry out an investigation of the dynamic bifurcation of the model.

## Existence of Periodic Solutions

The existence of periodic solutions, that is, Hopf points in the model is associated with a change in the equilibrium of singular points when a single pair of eigenvalues of the linearized system crosses the imaginary axis. The three-dimensional system has a Hopf bifurcation point when the Jacobean matrix has pure imaginary eigenvalues. The Jacobean matrix for this model is

$$J = \begin{bmatrix} f_{1\bar{S}} & f_{1\bar{X}_1} & f_{1\bar{X}_1} \\ f_{2\bar{S}} & f_{2\bar{X}_1} & f_{2\bar{X}_2} \\ f_{3\bar{S}} & f_{3\bar{X}_1} & f_{3\bar{X}_2} \end{bmatrix} \quad (34)$$

where $f_1$, $f_2$ and $f_3$ denote the lefthand sides of the mass balances (Eqs. 8–10). The eigenvalue $\lambda$ of the Jacobean matrix are the solutions of the characteristic matrix equation

$$-\lambda^3 + S_1\lambda^2 - S_2\lambda + S_3 = 0 \quad (35)$$

where $S_1$, $S_2$ and $S_3$ are the three invariants of $J$

$$S_1 = j_{11} + j_{22} + j_{33} \quad (36)$$

$$S_2 = \det\begin{pmatrix} j_{11} & j_{12} \\ j_{21} & j_{22} \end{pmatrix} + \det\begin{pmatrix} j_{22} & j_{23} \\ j_{32} & j_{33} \end{pmatrix} + \det\begin{pmatrix} j_{11} & j_{13} \\ j_{31} & j_{33} \end{pmatrix} \quad (37)$$

$$S_3 = \det(J) \quad (38)$$

The $j_{11}$, $j_{12}$, ... are the elements of $J$. The conditions of Hopf bifurcation in terms of the coefficients $S_1$, $S_2$, and $S_3$ can be derived by setting $\lambda = iw$ into Eq. 35 to yield

$$F_1 := S_1S_2 - S_3 = 0 \quad (39)$$

$$S_2 > 0 \quad (40)$$

The Jacobean terms are given explicitly by taking the derivatives of Eqs. 8–10, yielding

$$j_{11} = -1 - \bar{\theta}\left(\bar{X}_1\bar{r}_1' + \eta\bar{X}_2\bar{r}_2'\right), \quad j_{12} = -\bar{\theta}\bar{r}_1,$$

$$j_{13} = -\bar{\theta}\eta\bar{r}_2, \quad j_{21} = \bar{\theta}\bar{X}_1\bar{r}_1', \quad j_{22} = -W + \bar{r}_1\bar{\theta},$$

$$j_{23} = 0, \quad j_{31} = \bar{\theta}\bar{X}_2\bar{r}_2', \quad j_{32} = 0, \quad j_{33} = -W + \bar{r}_2\bar{\theta} \quad (41)$$

The first derivatives of $\bar{r}_i$ are given by Eq. 19. The simplest interactions between a Hopf point and a static limit point occur when the imaginary part of the complex conjugate eigenvalue pair goes to zero. This degeneracy, called the $F_1$ degeneracy, is defined by solving the steady-state equation ($F = 0$) (Eq. 14), the Hopf conditions (Eq. 39), and the static limit point conditions ($F_{\bar{S}} = 0$). Figures 7a–7c show the complete static and dynamic bifurcation diagrams in the parameter spaces ($\bar{S}_f$, $\bar{X}_{f_1}$), ($\bar{S}_f$, $\bar{X}_{f_2}$) and ($\bar{S}_f$, $W$). The boundaries of the double variety singularity are omitted from the analysis since they do not change the nature of the dynamic bifurcation of the model. When crossing the boundaries for the $F_1$ curve (indicated by a dash line), the number of Hopf points in the continuity diagrams increases/decreases by one. Moreover, it can be seen that the Hopf boundary and one of the boundaries of the hysteresis surface intersect. This adds in-

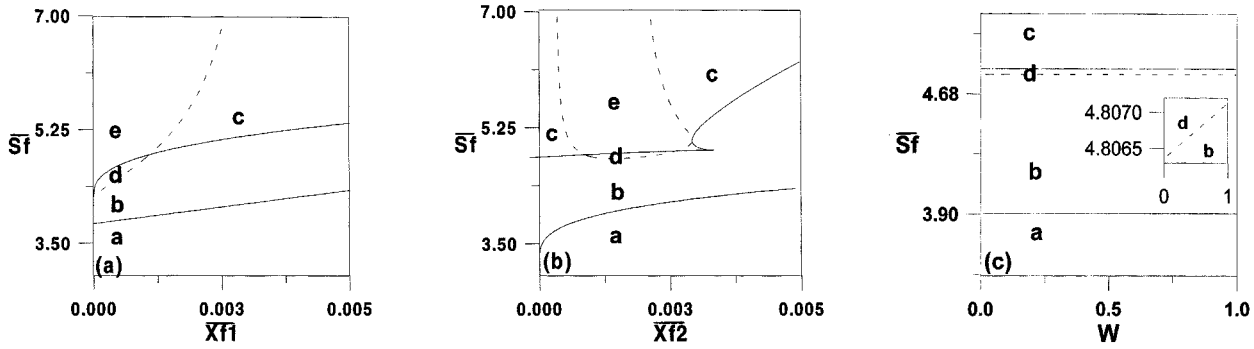


**Figure 7. Complete static and dynamic branch set.**

——: Hysteresis branch set; – – –: Hopf bifurcation curve.

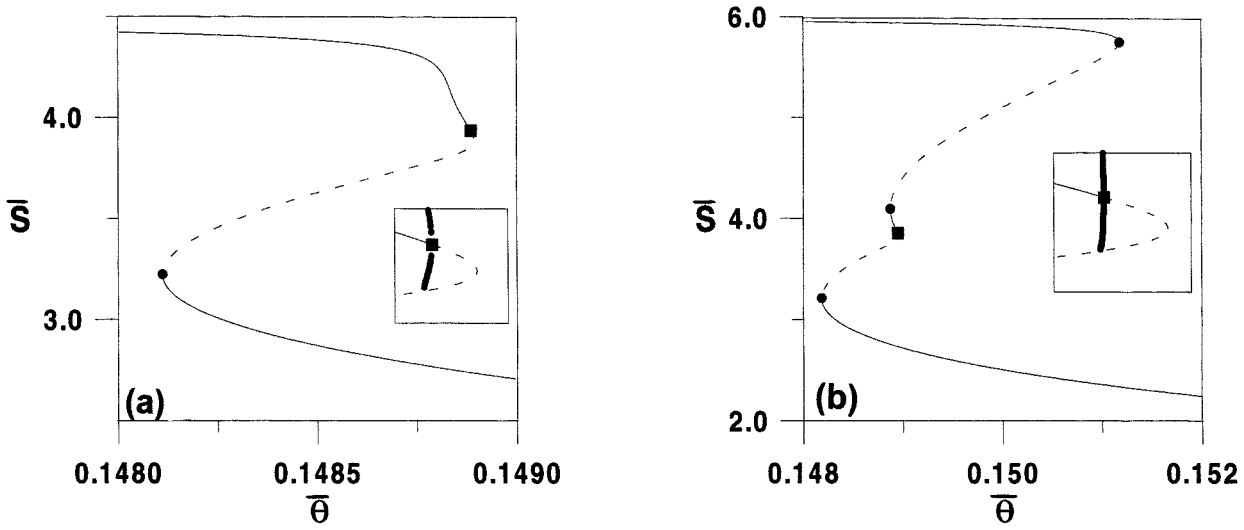


**Figure 8. Continuity diagrams for regions (d) and (e) of Figure 7a.**

(a) Hopf point (HB); static limit point (SLP); static limit point (SLP) in region (d). (b) SLP, SLP, HB, SLP, SLP in region (e). In both diagrams periodic branches emanating from the HB points (enlarged in the small diagrams) terminate homoclinically. ——: stable branch; – – –: unstable; ●: static limit point; ■: Hopf point; ——: periodic branch.

teresting features, as five different regions can be depicted in the system. Regions a, b, and c are unchanged. They are characterized, respectively, by no static limit point (SLP) or Hopf point (HB), two SLP and no HB, and four SLP with no HB. Region d is characterized on the other hand by the presence in this order of a Hopf point and two static limit points. Figure 8a shows an example of the continuity diagram for this region, obtained with $(\bar{S}_f, \bar{X}_{f_1}) = (4.4, 0.0002)$. Figure 8b shows, on the other hand, an example of the behavior expected in region e, obtained with $(\bar{S}_f, \bar{X}_{f_1}) = (5.6, 0.001)$. The system is characterized by the presence in this order of two static limit points, one Hopf point, and two static limit points. In both regions d and e homoclinic orbits can be found in the vicinity of the Hopf point as the periodic branches (enlarged in Figures 8a–8b) emanating from the HB terminate as they collide with the static branches. Moreover, the location of the periodic branch between static branches introduces the phenomenon of multistability in the system where self-sustained oscillations coexist with the high and low conversion static branch. Figures 9a–9c show time traces for the dilution rate of 6.71077 and operating conditions $(\bar{S}_f, \bar{X}_{f_1}, \bar{X}_{f_2}, W) = (8.0, 0.001, 0.001, 0.1)$ for three sets of initial conditions. The periodic behavior in this region is not orbitally stable since different initial conditions can break it and push it out of its domain of attraction, resulting in the annihilation of the oscillations. The same five modes of behavior can be seen in Figure 7b showing the effect of the other biomass feed ($\bar{X}_{f_2}$). As for the effect of the purge fraction shown in Figure 7c, it can be seen that only four modes of behavior exist. Mode e exists, but at physically unrealistic values of the purge fraction, that is, $W > 1$. The model, therefore, cannot predict more than three steady-state solutions without exhibiting bistability with self-sustained oscillations. Moreover, contrary to the static case, the Hopf boundary, enlarged in Figure 7c, increases with the purge fraction. The recycle ratio affects, therefore, the dynamic behavior of the system. Following changes in the purge fraction, the behavior of the bioreactor can move from region b to region d characterized by the presence of oscillations.

The analysis of the dynamic bifurcation for the case of nonsterile feed has revealed that the competing cultures can coexist in a state of limit cycle. The existence of oscillatory behavior in the model is due necessarily to the presence of inhibitory kinetics. In a later section we show that Monod kinetics cannot produce this behavior.

## Effect of Clean Feed Conditions

The interesting case of clean feed conditions can also be examined thoroughly using the singularity theory. When $\bar{X}_{f_1} = \bar{X}_{f_2} = 0$, Eqs. 12

$$\bar{X}_1 = \frac{\bar{X}_{f_1}}{W - \bar{r}_1\bar{\theta}}, \quad \bar{X}_2 = \frac{\bar{X}_{f_2}}{W - \bar{r}_2\bar{\theta}}$$

predicts two solutions. A trivial one $\bar{X}_1 = \bar{X}_2 = 0$ corresponds to wash out conditions $(\bar{S} = \bar{S}_f)$ and nontrivial solutions if either one of the following conditions are satisfied

$$\bar{r}_1 = \frac{W}{\bar{\theta}} \quad \text{or} \quad \bar{r}_2 = \frac{W}{\bar{\theta}} \tag{42}$$

Should the first condition alone be satisfied, that would correspond to $\bar{X}_1 \neq 0$ and similarly for the second condition. On the other hand, should the two conditions be simultaneously satisfied, then a coexistence of the two cultures is expected. Besides the wash-out line, the continuity diagram $(\bar{S}, \bar{\theta})$ admits two solutions, $\bar{X}_1 \neq 0$ and $\bar{X}_2 \neq 0$. The conditions of Eq. 42 define steady-state equations of order 2. Recasting the expression of $\bar{r}_1$ (Eq. 11), Eq. 42 yields

$$a\bar{S}^2 + b\bar{S} + c = 0 \tag{43}$$

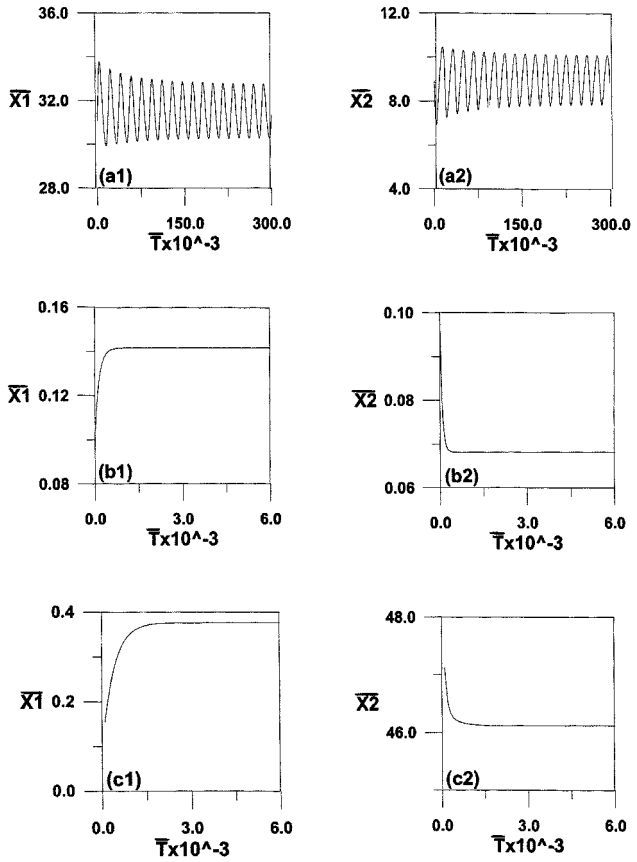


**Figure 9. Time traces showing multistability.**

(a) Period oscillations obtained with initial conditions ($\bar{S}$, $\bar{X}_{f_1}$, $\bar{X}_{f_2}$, $W$) = (3, 31, 9, 0.1); (b) low conversion attractor obtained with initial conditions ($\bar{S}$, $\bar{X}_{f_1}$, $\bar{X}_{f_2}$, $W$) = (1, 0.1, 0.1, 0.1); (c) high conversion attractor obtained with initial conditions ($\bar{S}$, $\bar{X}_{f_1}$, $\bar{X}_{f_2}$, $W$) = (1, 0.1, 50, 0.1).

with

$$a = \gamma_1, \quad b = 1 - \frac{\bar{\theta}}{W}, \quad c = 1 \tag{44}$$

For a quadratic function like Eq. 43, the singularity theory defines a simple bifurcation (codimension 0) defined by the following conditions

$$F = 0, \quad F_{\bar{S}} = 0 \quad \text{and} \quad F_{\bar{S}\bar{S}} \neq 0 \tag{45}$$

We recall from the previous section (Eq. 21) that the condition $F_{\bar{S}} = 0$ is satisfied only if

$$\gamma_1 \geq \frac{1}{\bar{S}_f^2} \quad \text{or} \quad \gamma_2 \geq \frac{\alpha}{\bar{S}_f^2} \tag{46}$$

Should either one of these conditions be satisfied, the equation $F_{\bar{S}} = 0$ defines one static limit point

$$\bar{S} = -\frac{b}{2a} \tag{47}$$

The condition $F_{\bar{S}\bar{S}} = 2a = 2\gamma_1$, on the other hand, vanishes only when the inhibition-constant $\gamma_1$ is zero. Substituting Eq. 47 into Eq. 43 yields

$$b^2 = 4ac \tag{48}$$

By recasting the expressions of $a$, $b$ and $c$ from Eq. 44, the condition of Eq. 48 defines the residence time $\bar{\theta}_{c1}$ at the static limit point

$$\bar{\theta}_{c1} = W\left(1 \pm 2\sqrt{\gamma_1}\right) \tag{49}$$

A similar analysis can be carried out for the case of $\bar{r}_2 = W/\theta$. This relation also yields a quadratic equation similar to Eq. 43 with

$$a = \gamma_2, \quad b = \left(1 - \frac{\theta\phi}{W}\right), \quad c = \alpha \tag{50}$$

The condition $F_{\bar{S}\bar{S}} = 0$ is violated only if $\gamma_2 = 0$. The residence time for this static limit point is defined by

$$\bar{\theta}_{c2} = \frac{W}{\phi}\left(1 \pm 2\sqrt{\gamma_2 \alpha}\right) \tag{51}$$

The relative location of the two curves $\bar{X}_1 \neq 0$ and $\bar{X}_2 \neq 0$ in the continuity diagram $(\bar{S}, \bar{\theta})$ depends on the location of the two limit points. The condition $\bar{\theta}_{c1} \leq \bar{\theta}_{c2}$ is equivalent to

$$\gamma_2 \geq \frac{1}{4\alpha}\left(\phi \pm 2\phi\sqrt{\gamma_1} - 1\right)^2 \tag{52}$$

This relation defines a boundary separating two modes of behavior, as will be seen later. Should none of the conditions of Eq. 46 be satisfied, then the continuity diagram $(\bar{S}, \bar{\theta})$ would not exhibit a static limit point. Wash-out conditions in this case are obtained by setting $\bar{S} = \bar{S}_f$ in Eqs. 42, respectively, leading to

$$\bar{\theta}_{c1} = \frac{W\left(1 + \bar{S}_f + \gamma_1 \bar{S}_f^2\right)}{\bar{S}_f} \tag{53}$$

and

$$\bar{\theta}_{c2} = \frac{W\left(\alpha + \bar{S}_f + \gamma_2 \bar{S}_f^2\right)}{\phi \bar{S}_f} \tag{54}$$

The coexistence of the two populations is possible if equations (Eq. 42) are simultaneously satisfied for some set of parameters. This is equivalent to the requirement that the specific growth rates should cross. Recasting the expression of $\bar{r}_1$ and $\bar{r}_2$ from Eq. 11 and eliminating $\theta$ from the two equations, it can be seen that the coexistence is possible if the following quadratic equation admits real roots $\bar{S}$

$$\bar{S}^2(\phi\gamma_1 - \gamma_2) + \bar{S}(\phi - 1) + (\phi - \alpha) = 0 \tag{55}$$

The discriminate

$$\Delta = (\phi - 1)^2 - 4(\phi\gamma_1 - \gamma_2)(\phi - \alpha) > 0 \qquad (56)$$

with either one of the roots satisfying

$$0 < \bar{S}_j = \frac{-(\phi - 1) \pm \sqrt{\Delta}}{2(\phi\gamma_1 - \gamma_2)} < \bar{S}_f \qquad (j = 1, 2) \qquad (57)$$

defines the boundary for the coexistence of the competing populations. The above results for the dynamics of clean feed conditions are summarized in Figure 10 in the parameter space $(\gamma_1, \gamma_2)$ for the values of $\alpha$, $\phi$ shown in Table 3 and for $\bar{S}_f = 6$. The solid line corresponds to Eqs. 56–57. A coexistence of the two populations is expected above this line. The dashed line corresponds to Eq. 52 defining the boundary for the relative location of the static limit points. To this are added the horizontal and vertical lines (Eq. 46) forming the boundaries for the existence of static limit points. A total of nine different stability regions are possible. The continuity diagrams expected in these regions are depicted in Figure 11a(i). In region a no static limit points exist and the continuity diagram (Figure 11a) is characterized by a Monod-like behavior. When crossing to region b, a static limit point appears in the continuity diagram (Figure 11b) but with no change in the stability. When crossing to region c, a static limit point appears but with a change in the stability in the branch ($\bar{X}_2 \neq 0$). In region d two limit points appear, one on each branch (Figure 11d). When crossing the solid line of Figure 10, the two curves ($\bar{X}_1 \neq 0$ and $\bar{X}_2 \neq 0$) necessarily intersect each other. Both regions (e–f) (Figures 11e–11f) are characterized by a crossing of the two curves, however, two static limit points appear in region f compared to one in e. Regions g and h are characterized by the crossing of the two curves and the presence of static limit points, however, wash-out conditions differ from those of regions e and f. Region i is the only region characterized by the crossing of the two curves, but with no static limit points (a Monod type behavior). Moreover, the diagrams (e, f, h) are characterized by the occurrence of bistability since the stable high conversion branch coexists with wash-out conditions. The dynamics in these regions are conditioned by startup conditions. Table 4 summarizes the different stability characteristics for the clean feed conditions.

### *Existence of periodic solutions for clean feed conditions*

In this section we investigate the existence of periodic solutions, that is, Hopf points for the case of clean feed conditions. We have seen that, for this case, the model admits a maximum of three steady-state solutions

$$\left(\bar{X}_1 = 0,\ \bar{X}_2 \neq 0\right), \qquad (58a)$$

$$\left(\bar{X}_1 \neq 0,\ \bar{X}_2 = 0\right), \qquad (58b)$$

$$\left(\bar{X}_1 \neq 0,\ \bar{X}_2 \neq 0\right), \qquad (58c)$$

The first case corresponds necessarily to $W - \bar{r}_1\bar{\theta} \neq 0$ and $W - \bar{r}_2\bar{\theta} = 0$. The Jacobean of the system (Eq. 41) is reduced

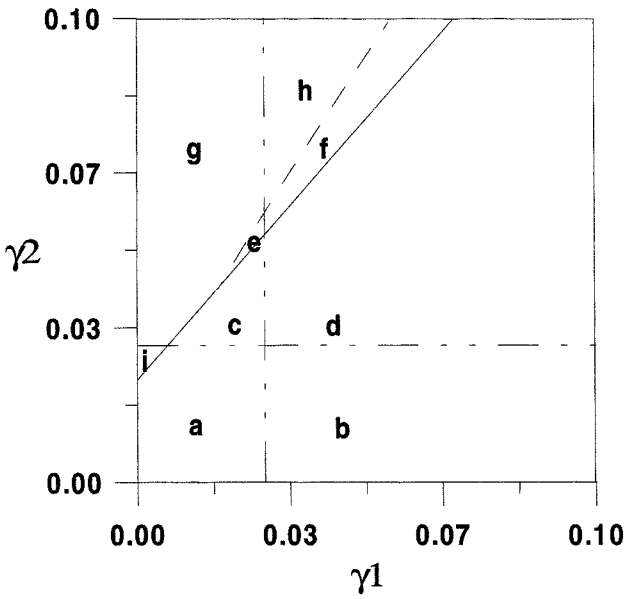


**Figure 10. Branch set for the clean feed conditions.**

——: Boundary for the coexistence of the two populations; – – –: boundary for the relative location of static limit points of curves ($\bar{X}_1 \neq 0$) and ($\bar{X}_2 \neq 0$); horizontal and vertical dash lines are boundaries for the existence of static limit points.

to

$$J = \begin{bmatrix} j_{11} & j_{12} & j_{13} \\ 0 & j_{22} & 0 \\ j_{31} & 0 & 0 \end{bmatrix} \qquad (59)$$

It is easy to check that the eigenvalues $\lambda$ of the Jacobean satisfy

$$(j_{22} - \lambda)\left(\lambda^2 - \lambda j_{11} - j_{13}j_{31}\right) = 0 \qquad (60)$$

The first eigenvalue $\lambda = j_{22}$ is real. For the quadratic equation to admit pure imaginary eigenvalues, it is necessary to have

$$j_{11} = 0 \quad \text{and} \quad j_{13}j_{31} < 0 \qquad (61)$$

However, since $\bar{X}_1 = 0$, Eq. 41 yields $j_{11} = -1 - \eta j_{31}$. Therefore, $j_{31} = -1/\eta$. The product $j_{13}j_{31}$ is equal to $-\theta\eta r_2(-1/\eta) = \theta r_2$, which is always positive. This violates the condition of Eq. 61. Therefore, no Hopf point can be expected in the model. A similar analysis can be carried out for the case of ($\bar{X}_1 \neq 0$, $\bar{X}_2 = 0$).

The third, theoretical solution corresponds to condition c of Eq. 58, which is also equivalent to

$$-W + \bar{r}_1\bar{\theta} = 0 \quad \text{and} \quad -W + \bar{r}_2\bar{\theta} = 0 \qquad (62)$$

The Jacobean in this case is reduced to

$$J = \begin{bmatrix} j_{11} & j_{12} & j_{13} \\ j_{21} & 0 & 0 \\ j_{31} & 0 & 0 \end{bmatrix} \qquad (63)$$

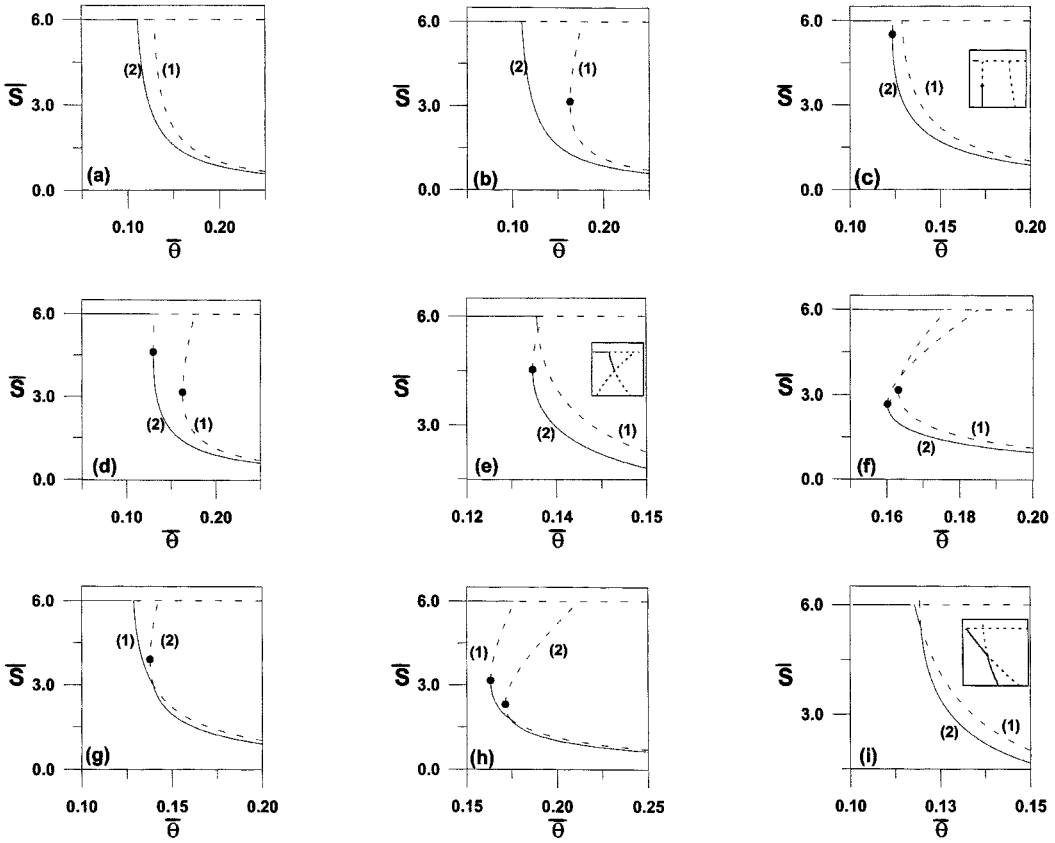


**Figure 11. Continuity diagrams for the different regions of Figure 10.**

——: Stable branch; – – –: unstable; ●: static limit point; (1) indicates the branch $\bar{X}_1 \neq 0$; (2) indicates the branch $\bar{X}_2 \neq 0$.

The eigenvalues $\lambda$ satisfy

$$\lambda = 0 \quad \text{or} \quad \left(\lambda^2 - \lambda j_{11} - j_{21} j_{12} - j_{31} j_{13}\right) = 0 \qquad (64)$$

For the quadratic equation to admit pure nonzero imaginary eigenvalues, it is necessary to have

$$j_{11} = 0 \quad \text{and} \quad j_{21} j_{12} + j_{31} j_{13} < 0 \qquad (65)$$

However, it can be noted using Eqs. 41 and 62 that $j_{12} = -W$ and $j_{13} = -\eta W$. The condition of Eq. 65 is then equivalent to $j_{21} + \eta j_{31} > 0$. However, it can be seen from Eq. 41 that $j_{11} = -1 - j_{21} - \eta j_{31}$. Since $j_{11} = 0$, this results in $j_{21} + \eta j_{31} = -1$ which contradicts the condition of Eq. 65.

The analysis in this section was carried out without reference to the explicit expression of the growth expressions. We conclude, therefore, that the model used for the CSTBR cannot exhibit periodic behavior for the case of clean feed conditions regardless of the growth kinetics model.

## Noninhibitory Kinetics Model

The investigation carried out so far with the Andrew's inhibitory kinetics can be used to recover the bifurcation mechanism for the case of the noninhibitory (Monod) growth

**Table 4. Stability Characteristics for Regions of Clean Feed Conditions for Andrew's Growth Kinetics**

| Region | Curve 1 ($\bar{X}_1 \neq 0$) | Curve 2 ($\bar{X}_2 \neq 0$) | Coexistence | Wash-Out Conditions | Bistability |
|---|---|---|---|---|---|
| *a* | $BR_W$ | $BR_W$ | *N* | Eq. 54 | *N* |
| *b* | *SLP*, $BR_W$ | $BR_W$ | *N* | Eq. 54 | *N* |
| *c* | $BR_W$ | *SLP*, $BR_W$ | *N* | Eq. 51 | *N* |
| *d* | *SLP*, $BR_W$ | *SLP*, $BR_W$ | *N* | Eq. 51 | *N* |
| *e* | $BR_I$, $BR_W$ | *SLP*, $BR_I$, $BR_W$ | *Y* | Eq. 51 | *Y* |
| *f* | *SLP*, $BR_I$, $BR_W$ | *SLP*, $BR_I$, $BR_W$ | *Y* | Eq. 51 | *Y* |
| *g* | $BR_I$, $BR_W$ | $BR_I$, *SLP*, $BR_W$ | *Y* | Eq. 53 | *N* |
| *h* | $BR_I$, *SLP*, $BR_W$ | $BR_I$, *SLP*, $BR_W$ | *Y* | Eq. 49 | *Y* |
| *i* | $BR_I$, $BR_W$ | $BR_I$, $BR_W$ | *Y* | Eq. 53 | *N* |

kinetics model. As the dimensionless inhibition constants $\gamma_1$ and $\gamma_2$ go to zero, the specific growth rates (Eq. 11) become

$$\bar{r}_1 = \frac{\bar{S}}{1+\bar{S}} \quad \text{and} \quad \bar{r}_2 = \frac{\phi\bar{S}}{\alpha+\bar{S}} \tag{66}$$

Recasting the expression of $F_{\bar{S}}$ (Eq. 18) yields

$$-F_{\bar{S}} = +1+\bar{\theta}^2\bar{X}_{f_1}\frac{\bar{r}_1'}{\left(W-\bar{r}_1\bar{\theta}\right)^2}+\eta\bar{\theta}^2\bar{X}_{f_2}\frac{\bar{r}_2'}{\left(W-\bar{r}_2\bar{\theta}\right)^2} \tag{67}$$

with

$$\bar{r}_1' = \frac{1}{(1+\bar{S})^2} \quad \text{and} \quad \bar{r}_2' = \frac{\phi\alpha}{(\alpha+\bar{S})^2} \tag{68}$$

These two terms are positive; hence, all the terms in $F_{\bar{S}}$ are positive. The condition $F_{\bar{S}}=0$ is thus never satisfied and the model will always predict a unique solution.

For the case of clean feed conditions, the continuity diagram $(\bar{S},\bar{\theta})$ is also characterized by the presence of wash-out conditions line and the two solutions $\bar{X}_1 \neq 0$ and $\bar{X}_2 \neq 0$. Wash-out conditions occur for any value of $\bar{\theta}$ less than the critical values of residence times obtained by setting $\bar{S}=\bar{S}_f$ in Eq. 42,

$$\bar{\theta}_{c1} = \frac{W\left(1+\bar{S}_f\right)}{\bar{S}_f} \tag{69}$$

$$\bar{\theta}_{c2} = \frac{W\left(\alpha+\bar{S}_f\right)}{\phi\bar{S}_f} \tag{70}$$

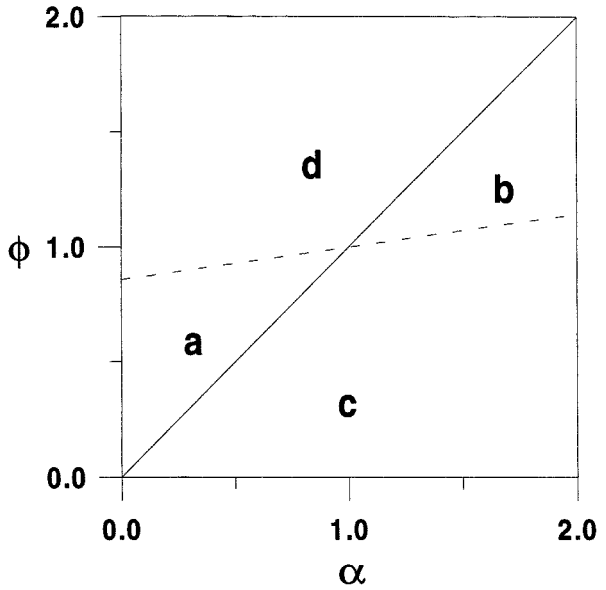


**Figure 12. Branch set for the dynamics of the reactor for clean feed conditions and Monod kinetics.**

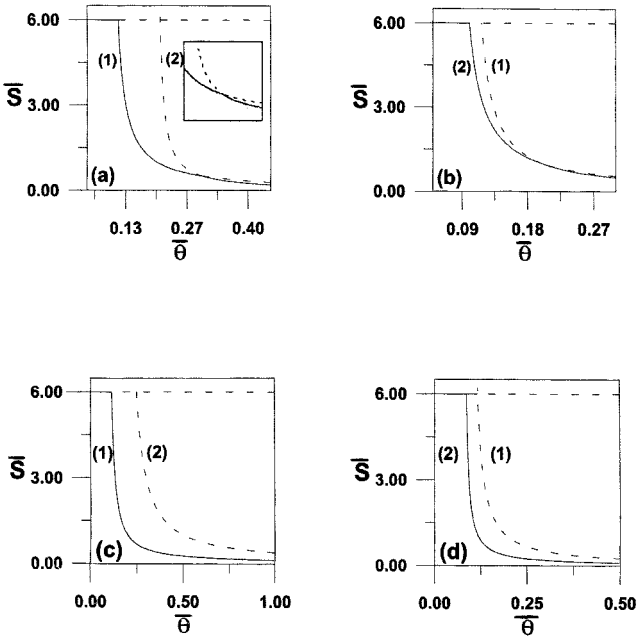


**Figure 13. Continuity diagrams for the different regions of Figure 12.**

——: Stable branch; – – –: unstable; (1) indicates the branch $\bar{X}_1 \neq 0$; (2) indicates the branch $\bar{X}_2 \neq 0$.

The condition $\bar{\theta}_{c1} < \bar{\theta}_{c2}$ defines one boundary for the problem. The coexistence of the two populations is satisfied when the specific growth rates intersect (Eq. 42). This occurs at the substrate concentration

$$\bar{S} = \frac{\alpha-\phi}{\phi-1} \tag{71}$$

and at residence time

$$\bar{\theta} = \frac{(\alpha-1)W}{\alpha-\phi} \tag{72}$$

This coexistence is conditioned by the positivity of the term $(\alpha-\phi)(\phi-1)$. The condition $0<(\alpha-\phi)/(\phi-1)\leq\bar{S}_f$ defines another boundary for the problem. Figure 12 summarizes these results in the parameter space $(\phi,\alpha)$ for $\bar{S}_f=6$. A total of four different regions are expected in the system (Figures 13a–13d). Regions a and b are characterized by the crossing of the two curves but with different stability behavior. The branch $\bar{X}_1 \neq 0$ is stable in region a, while it is unstable in region b. Regions c and d are characterized, on the other hand, by no crossing, but also with different stability behavior for the two curves. Table 5 summarizes the different stability characteristics for clean feed conditions with Monod growth kinetics.

### *Existence of periodic solutions for Monod's kinetics*

In this section we analyze whether Monod kinetics alone are capable of producing an oscillatory behavior in the model. Recasting the conditions (Eqs. 39–40) for the existence of a

**Table 5. Stability Characteristics for Regions of Clean Feed Conditions for Monod Growth Kinetics**

| Region | Curve 1 ($\bar{X}_1 \neq 0$) | Curve 2 ($\bar{X}_2 \neq 0$) | Coexistence | Wash-Out Conditions |
|---|---|---|---|---|
| *a* | $BR_I$, $BR_W$ | $BR_I$, $BR_W$ | *Y* | Eq. 69 |
| *b* | $BR_I$, $BR_W$ | $BR_I$, $BR_W$ | *Y* | Eq. 70 |
| *c* | $BR_W$ | $BR_W$ | *N* | Eq. 69 |
| *d* | $BR_W$ | $BR_W$ | *N* | Eq. 70 |

Hopf point and noting that the first derivative of the growth rates $\bar{r}_1'$ and $\bar{r}_2'$ (Eqs. 68) can be related to $\bar{r}_1$ and $\bar{r}_2$ (Eqs. 66) by

$$\bar{r}_1' = \frac{\bar{r}_1^2}{\bar{S}^2} \quad \text{and} \quad \bar{r}_2' = \frac{\alpha \bar{r}_2^2}{\phi \bar{S}^2} \tag{73}$$

Noting also that, at the stationary point, the two components $j_{22}$ and $j_{33}$ (Eq. 41) are equal, using Eqs. 12 to

$$j_{22} = -\frac{\bar{X}_{1f}}{\bar{X}_1} \qquad j_{33} = -\frac{\bar{X}_{2f}}{\bar{X}_2} \tag{74}$$

Under this condition, the Hopf conditions of Eqs. 39–40 can be evaluated analytically. The resulting expressions, obtained using the software MATHEMATICA (1992) are given in the Appendix. It can be seen that the term $S_2$ is composed only of positive terms. Eliminating the clean feed cases and the nonrealistic case of $\bar{\theta} = 0$, the second Hopf condition $S_2 > 0$ is therefore always satisfied. The term $-F_1 := -(S_1 S_2 - S_3)$ is also only composed of positive terms. It can therefore never vanish, barring the nonrealistic case of $\bar{\theta} = 0$. We conclude then that the first Hopf condition (Eq. 39) can never be satisfied, and therefore Monod kinetics cannot produce an oscillatory behavior in the system.

## Conclusions

The stability characteristics of a bioreactor with cell recycle where two microbial populations are engaged in a pure and simple competition have been studied, using the singularity theory. The analysis of static bifurcation for nonsterile feed has shown that the hysteresis is the singularity of the highest order the model can predict. The model can exhibit for any combination of parameters either unique, three, or a maximum five steady-state solutions. The analysis of dynamic bifurcation for the nonsterile feed has revealed that the two competing cultures can coexist in a state of limit cycle for a wide range of parameters. However, these self-sustained oscillations are not orbitally stable and any variations in the feed conditions can annihilate them and bring the system to a stable steady state. The effect of substrate feed, biomass feed, and recycle ratio on the relative location of point and limit cycle attractors was studied. While the recycle ratio has no effect on the static behavior, it can affect the existence of oscillatory behavior in the model.

For the case of clean feed, the use of the singularity theory was helpful in drawing a general stability diagram where nine different stability behavior of the competing populations were delineated. Among them are five regions where the coexistence at discrete values of the dilution rate is satisfied. For each of the found behaviors, analytical conditions for the coexistence of the competing cultures and for the occurrence of wash-out conditions were established. Moreover, a simple analysis of the dynamic bifurcation has shown that oscillations cannot exist under clean feed conditions, regardless of the chosen growth kinetics expressions.

The general treatment offered by the theory has been used to recover the stability characteristics with Monod kinetics, as a limiting case of the inhibitory model. Four different stability diagrams were obtained with clean feed conditions. Among them are two regions where the conditions of the coexistence are satisfied. Finally, an analysis of the conditions of existence of self-sustained oscillations has revealed that inhibitory kinetics are necessary for the occurrence of oscillations and that Monod kinetics cannot produce an oscillatory behavior.

## Notation

$K_{I_j}$ = substrate inhibition constants in specific growth rates $r_j$ ($j = 1, 2$) (mass volume$^{-1}$)
$K_j$ = constant in the specific growth rates $r_j$ ($j = 1, 2$) (volume mass$^{-1}$)
$Q$ = volumetric flow rate (volume time$^{-1}$)
$r_j$ = specific growth rates of population $j$ ($j = 1, 2$) (time$^{-1}$)
$R$ = recycle ratio
$S$ = concentration of substrate $S$ (mass volume$^{-1}$)
$t$ = time
$V$ = reactor volume (volume)
$W$ = fraction of $Q$ purged from the reactor
$X_j$ = biomass concentration of species $j$ (mass volume$^{-1}$)
$Y_j$ = yield coefficient of species $j$ ($j = 1, 2$) (mass$_{X_j}$ mass$_S^{-1}$)
$\alpha$ = dimensionless constant in $\bar{r}_2$
$\eta$ = ratio of yield coefficient ($Y_1/Y_2$)
$\phi$ = dimensionless constant in $\bar{r}_2$

### *Subscripts*

$f$ = feed
$R$ = recycle
$(\bar{\cdot})$ = dimensionless value of $(\cdot)$

### *Abbreviations*

$BR_W$ = bifurcation point corresponding to the intersection with wash-out conditions line
$BR_I$ = bifurcation point corresponding to the crossing of curves ($X_1 \neq 0$) and ($X_2 \neq 0$)
$HB$ = Hopf bifurcation point
$SLP$ = static limit point

## Literature Cited


Agrawal, P., C. Lee, H. C. Lim, and D. Ramkrishma, "Theoretical Investigations of Dynamic Behavior of Isothermal Continuous Stirred Tank Biological Reactors," *Chem. Eng. Sci.*, **37**, 453 (1982).

Ajbar, A., and G. Ibrahim, "Stability and Bifurcation of an Unstructured Model of a Bioreactor with Cell Recycle," *Math. Comput. Modeling*, **25**, 31 (1997).

Ajbar, A., and G. Ibrahim, "Periodic and Nonperiodic Oscillatory Behavior in a Model for Activated Sludge Reactors," *Math. Comput. Modeling*, **25**, 9 (1997).

Alhumaizi, K., and R. Aris, *Surveying Dynamical System: A Study of the Gray-Scott Reaction in a Two-Phase Reactor*, Longman, London, England (1995).

Andrews, J. F., "A Mathematical Model for the Continuous Culture of Microorganisms Utilizing Substrates," *Biotechnol. Bioeng.*, **10**, 707 (1968).

Aris, R., and A. E. Humphrey, "Dynamics of a Chemostat in Which Two Organisms Compete for a Common Substrate," *Biotechnol. Bioeng.*, **19**, 1375 (1977).

Balakotaiah, V., and D. Luss, "Structure of the Steady State Solutions of Lumped Parameter Chemically Reacting System," *Chem. Eng. Sci.*, **37**, 1611 (1982).
Baltzis, B. C., and A. G. Fredrickson, "Competition of Two Microbial Populations for a Single Source in a Chemostat When One of Them Exhibits Wall Attachment," *Biotechnol. Bioeng.*, **25**, 2419 (1983).
Baltzis, B. C., and A. G. Fredrickson, "Coexistence of Two Microbial Populations Competing for a Renewable Resource in a Non-Predator-Prey System," *Bull. Math. Biol.*, **46**, 155 (1984).
Baltzis, B. C., G. A. Lewandowski, S. H. Chang, and Y. F. Ko, "Fill-and-Draw Reactor Dynamics in Biological Treatment of Hazardous Wastes," *Biotechnology Applications in Hazardous Waste Treatment*, G. A. Lewandowski, P. M. Armenante, and B. C. Baltzis, eds., Engineering Foundation, New York, p. 111 (1989).
Bertucco, A., P. Volpe, H. E. Klei, T. F. Anderson, and D. W. Sundstrom, "The Stability of Activated Sludge Reactors with Substrate Inhibition Kinetics and Solids Recycle," *Water Res.*, **36**, 9 (1989).
Butler, G. J., and G. S. K. Wolkowicz, "A Mathematical Model of the Chemostat with a General Class of Functions Describing Nutrient Uptake," *SIAM J. Appl. Math.*, **45**, 138 (1985).
D'anna, H., P. G. Lingola, and S. K. Scott, "The Application of Singularity Theory to Isothermal Autocatalytic Systems: The Elementary Scheme $A + mB \rightarrow (m+1)B$," *Proc. R. Soc. Lond.*, **A403**, 341 (1986).
DiBiasio, D., H. C. Lim, and W. A. Weigand, "An Experimental Investigation of Stability and Multiplicity of Steady-States in a Biological Reactor," *AIChE J.*, **27**, 284 (1981).
Dikshitulu, S., B. C. Baltzis, G. A. Lewandowski, and S. Pavlou, "Competition Between Two Microbial Populations in a Sequencing Fed-Batch Reactor: Theory, Experimental Verification and Implications for Waste Treatment Applications," *Biotechnol. Bioeng.*, **42**, 643 (1993).
Doedel, E. J., and J. P. Kernevez, *Auto: Software for Continuation and Bifurcation Problems in Ordinary Differential Equations*, California Institute of Technology, Pasadena, CA (1986).
Fredrickson, A. G., and G. N. Stephanopoulos, "Microbial Competition," *Science*, **213**, 972 (1981).
Golubitsky, M., and D. Schaeffer, *Singularities and Groups in Bifurcation Theory*, Vol. 1, Springer-Verlag, New York (1985).
Hale, J. K., and A. S. Somolinos, "Competition for Fluctuating Nutrient," *J. Math. Biol.*, **18**, 255 (1983).
Hansen, S. R., and S. P. Hubbell, "Single-Nutrient Microbial Competition: Qualitative Agreement Between Experimental and Theoretically Forecast Outcomes," *Science*, **207**, 1491 (1980).
Hsu, S. B., "Limiting Behavior for Competing Species," *SIAM J. Appl. Math.*, **34**, 760 (1978).
Hsu, S. B., "A Competition Model for a Seasonally Fluctuating Nutrient," *J. Math. Biol.*, **9**, 115 (1980).
Lenas, P., and S. Pavlou, "Chaotic Response of a Periodically Forced System of Two Competing Microbial Species," *Chaotic Dynamics: Theory and Practice*, T. C. Bountis, ed., Plenum, New York, p. 283 (1992).
MATHEMATICA, Wolfram Research, Inc. (1992).
Matsubara, M., N. Watanabe, and S. Hasegawa, "Bifurcations in a Bang-Bang Controlled Mixed Culture," *Chem. Eng. Sci.*, **41**, 523 (1986).
Pavlou, S., I. G. Kevrekidis, and G. Lyberatos, "On the Coexistence of Competing Species in a Chemostat under Cycling," *Biotechnol. Bioeng.*, **35**, 224 (1990).
Pavlou, S., and I. G. Kevrekidis, "Microbial Predation in a Periodically Operated Chemostat: A Global Study of the Interaction Between Natural and Externally Imposed Frequencies," *Math. Biosci.*, **108**, 1 (1992).
Powell, G. E., "Structured Instability of the Theory of Simple Competition," *J. Theor. Biol.*, **18**, 259 (1988).
Smith, H. L., and P. Waltman, *The Theory of the Chemostat. Dynamics of Microbial Competition*, Cambridge Studies in Mathematical Biology, Cambridge University Press, London (1995).
Stephanopoulos, G., R. Aris, and A. G. Fredrickson, "A Stochastic Analysis of the Growth of Competing Microbial Populations in a Continuous Biochemical Reactor," *Math. Biosci.*, **45**, 99 (1979).
Stephanopoulos, G., A. G. Fredrickson, and R. Aris, "The Growth of Competing Microbial Populations in a CSTR with Periodically Varying Inputs," *AIChE J.*, **25**, 863 (1979).

## Appendix: Analytical Expressions of the Hopf Conditions for Monod's Kinetics

$$S_2 = \frac{\bar{r}_1^2\bar{\theta}\bar{X}_{f_1}}{\bar{S}^2} + \frac{\alpha\eta\bar{r}_2^2\bar{\theta}\bar{X}_{f_2}}{\phi\bar{S}^2} + \frac{\bar{X}_{f_1}}{\bar{X}_1} + \frac{\bar{r}_1^3\bar{\theta}^2\bar{X}_1}{\bar{S}^2} + \frac{\bar{X}_{f_2}}{\bar{X}_2}$$

$$+ \frac{\bar{X}_{f_1}\bar{X}_{f_2}}{\bar{X}_1\bar{X}_2} + \frac{\bar{r}_1^2\bar{\theta}\bar{X}_{f_2}\bar{X}_1}{\bar{S}^2\bar{X}_2} + \frac{\alpha\eta\bar{r}_2^3\bar{\theta}^2\bar{X}_2}{\phi\bar{S}^2} + \frac{\alpha\eta\bar{r}_2^2\bar{\theta}\bar{X}_{f_1}\bar{X}_2}{\phi\bar{S}^2\bar{X}_1}$$

$$-F_1 := + \frac{2\bar{r}_1^2\bar{\theta}\bar{X}_{f_1}}{\bar{S}^2} + \frac{\bar{r}_1^3\theta^2\bar{X}_{f_1}}{\bar{S}^2} + \frac{2\alpha\eta\bar{r}_2^2\bar{\theta}\bar{X}_{f_2}}{\phi\bar{S}^2} + \frac{\alpha\eta\bar{r}_2^3\bar{\theta}^2\bar{X}_{f_2}}{\phi\bar{S}^2}$$

$$+ \frac{\bar{X}_{f_1}^2}{\bar{X}_1^2} + \frac{\bar{X}_{f_1}}{\bar{X}_1} + \frac{\bar{r}_1^2\bar{\theta}\bar{X}_{f_1}^2}{\bar{S}^2\bar{X}_1} + \frac{2\alpha\eta\bar{r}_2^2\bar{\theta}\bar{X}_{f_1}\bar{X}_{f_2}}{\phi\bar{S}^2\bar{X}_1} + \frac{\bar{r}_1^3\bar{\theta}^2\bar{X}_1}{\bar{S}^2}$$

$$+ \frac{\bar{r}_1^4\bar{\theta}^2\bar{X}_{f_1}\bar{X}_1}{\bar{S}^4} + \frac{2\alpha\eta\bar{r}_1^2\bar{r}_2^2\bar{\theta}^2\bar{X}_{f_2}\bar{X}_1}{\phi\bar{S}^4} + \frac{\bar{r}_1^5\bar{\theta}^3\bar{X}_1^2}{\bar{S}^4} + \frac{\bar{X}_{f_2}^2}{\bar{X}_2^2}$$

$$+ \frac{\bar{X}_{f_1}\bar{X}_{f_2}^2}{\bar{X}_1\bar{X}_2^2} + \frac{\bar{r}_1^2\bar{\theta}\bar{X}_{f_2}^2\bar{X}_1}{\bar{S}^2\bar{X}_2^2} + \frac{\bar{X}_{f_2}}{\bar{X}_2} + \frac{2\bar{r}_1^2\bar{\theta}\bar{X}_{f_1}\bar{X}_{f_2}}{\bar{S}^2\bar{X}_2}$$

$$+ \frac{\alpha\eta\bar{r}_2^2\bar{\theta}\bar{X}_{f_2}^2}{\phi\bar{S}^2\bar{X}_2} + \frac{\bar{X}_{f_1}^2\bar{X}_{f_2}}{\bar{X}_1^2\bar{X}_2} + \frac{2\bar{X}_{f_1}\bar{X}_{f_2}}{\bar{X}_1\bar{X}_2} + \frac{2\bar{r}_1^2\bar{\theta}\bar{X}_{f_2}\bar{X}_1}{\bar{S}^2\bar{X}_2}$$

$$+ \frac{\bar{r}_1^4\bar{\theta}^2\bar{X}_{f_2}\bar{X}_1^2}{\bar{S}^4\bar{X}_2} + \frac{\alpha\eta\bar{r}_2^3\bar{\theta}^2\bar{X}_2}{\phi\bar{S}^2} + \frac{2\alpha\eta\bar{r}_1^2\bar{r}_2^2\bar{\theta}^2\bar{X}_{f_1}\bar{X}_2}{\phi\bar{S}^4}$$

$$+ \frac{\alpha^2\eta^2\bar{r}_2^4\bar{\theta}^2\bar{X}_{f_2}\bar{X}_2}{\phi^2\bar{S}^4} + \frac{\alpha\eta\bar{r}_2^2\bar{\theta}\bar{X}_{f_1}^2\bar{X}_2}{\phi\bar{S}^2\bar{X}_1^2} + \frac{2\alpha\eta\bar{r}_2^2\bar{\theta}\bar{X}_{f_1}\bar{X}_2}{\phi\bar{S}^2\bar{X}_1}$$

$$+ \frac{\alpha\eta\bar{r}_1^3\bar{r}_2^2\bar{\theta}^3\bar{X}_1\bar{X}_2}{\phi\bar{S}^4} + \frac{\alpha\eta\bar{r}_1^2\bar{r}_2^3\bar{\theta}^3\bar{X}_1\bar{X}_2}{\phi\bar{S}^4} + \frac{\alpha^2\eta^2\bar{r}_2^5\bar{\theta}^3\bar{X}_2^2}{\phi^2\bar{S}^4}$$

$$+ \frac{\alpha^2\eta^2\bar{r}_2^4\bar{\theta}^2\bar{X}_{f_1}\bar{X}_2^2}{\phi^2\bar{S}^4\bar{X}_1}$$

*Manuscript received Mar. 16, 1999, and revision received Aug. 26, 1999.*